Remarkable variability of dyke features at the Vicuña Pampa Volcanic Complex, Southern Central Andes

Silvina Guzmán, Marco Neri, Roberto Carniel, Joan Martí, Pablo Grosse, Carolina Montero-López, Adelina Geyer

DR. SILVINA GUZMAN (Orcid ID : 0000-0003-3632-2960)
DR. MARCO NERI (Orcid ID : 0000-0002-5890-3398)
DR. CAROLINA MONTERO-LÓPEZ (Orcid ID : 0000-0002-3943-5648)

Article type : Paper

Reference number: TER-2016-0055.R2
Received date: 17-May-2016
Revised version received date: 31-Mar-2017
Accepted date: 06-Apr-2017

Remarkable variability of dyke features at the Vicuña Pampa Volcanic Complex, Southern Central Andes

Silvina Guzmán[1,2], Marco Neri[3], Roberto Carniel[4], Joan Martí[2, a], Pablo Grosse[5], Carolina Montero-López[1], Adelina Geyer[2]

[1] Instituto de Bio y Geociencias del NOA (IBIGEO), UNSa, CONICET, 9 de Julio 14, 4405, Rosario de Lerma, Salta, Argentina

[2] Institute of Earth Sciences Jaume Almera, ICTJA-CSIC, Lluis Sole i Sabaris s/n, 08028 Barcelona, Spain

[3] Istituto Nazionale di Geofisica e Vulcanologia, Osservatorio Etneo-Sezione di Catania, Piazza Roma, 2 – 95123 Catania, Italy

[4] Laboratorio di misure e trattamento dei segnali, Dipartimento Politecnico di Ingegneria e Architettura

(DPIA) Università di Udine, Via delle Scienze, 206 - 33100 Udine, Friuli, Italy
[5] CONICET and Fundación Miguel Lillo, Miguel Lillo 251, 4000 Tucumán, Argentina

[a] Now at the Institut des Sciences de la Terre d'Orleans (ISTO, CNRS), Université d'Orleans, Campus Géosciences, 1A rue de la Férolerie, F45071, Orleans Cedex 2, France

Corresponding Author

Silvina Guzmán
Permanent address: Instituto de Bio y Geociencias del NOA (IBIGEO), CONICET-UNSa, 9 de Julio 14 (4405), Rosario de Lerma, Salta, Argentina, sguzman@conicet.gov.ar; Tel: +54 387 4931755

Short title: Remarkable variability of dyke features

Abstract

Dykes at the Vicuña Pampa Volcanic Complex, which are mostly basaltic (trachy)-andesite and (trachy)-andesite, are exposed at the base and along the walls of a large depression resulting from intense degradation. Dykes intruding stiff layers (lavas, plugs and necks) are thin, mostly dip >60° and have coherent textures, whereas dykes intruding more compliant materials (breccias and conglomerates) tend to be thicker, have lower dips and have coherent, brecciated or mixed textures (coherent and brecciated textural domains in a single or compound dyke). Single dykes with brecciated and mixed textures are only found intruding near-surface units. Dykes with mixed textures always have sharp contacts between domains. Dykes with sinuous domain contacts and enclaves of one domain inside the other are interpreted as resulting from dyke arrest, partial cooling and reinjection of new magma. Dykes with straight domain contacts are

considered to be compound dykes, with a new dyke intruding along the margins of an older, solidified one.

Keywords: dykes, dyke textures, volcanic massif, Vicuña Pampa, Central Andes

Introduction

In recent decades, several studies have investigated dyke propagation by focusing on their field characteristics or following a modelling approach (experimental, numerical, analytical and/or analogue). Many of these studies analyze the influence on dyke emplacement of the physical parameters of both host rock and intruding magma. Dyke thickness is highly dependent on the local stresses along the potential dyke path (load of the volcanic edifice above the dyke, depth and distance from the edifice; e.g. Pinel and Jaupart, 2000) and on the stiffness (Young's modulus, "E") of the medium they traverse, with thicker dykes found in more compliant host rocks (e.g. Gudmundsson *et al.*, 2012; Delcamp *et al*., 2012; Geshi and Neri, 2014). Dyke dip is also found to be deflected or arrested at the contact between layers (Gudmundsson, 2011; Browning and Gudmundsson, 2015). When crossing layers of similar stiffness, or when the upper layer is more compliant, the dyke changes from more to less vertical; however, when the upper layer is stiffer, the dyke tends to be deflected to form a sill (Gudmundsson, 2011). Although there are several studies focusing on the field characteristics of dykes (e.g. Ferrari *et al.*, 1991; Gautneb and Gudmundsson, 1992; Gudmundsson, 1995; Gudmundsson and Brenner, 2005; Goto *et al.,* 2008; Kavanagh and Sparks, 2011; Delcamp *et al*., 2012; Daniels *et al.*, 2012; Gudmundsson *et al*., 2012; Petronis *et al.*, 2013; Geshi and Oikawa, 2014; Geshi and Neri, 2014;

Vezzoli and Corazzato, 2016), most are focused on their geometrical features; their textural patterns have received much less attention (e.g. Ferrari *et al.*, 1991; Gautneb and Gudmundsson, 1992; Goto *et al.,* 2008; Gudmundsson *et al*., 2012; Petronis *et al.*, 2013; Geshi and Oikawa, 2014; Geshi and Neri, 2014; Vezzoli and Corazzato, 2016). However, textures can provide information on the dyke's emplacement history. They can provide information on the rheological, mechanical and/or thermal contrasts between the intruding magma and the host rock (magma viscosity, crystal segregation, magma rheology, host-rock mechanical properties, local stress fields, depth of emplacement, differences in temperature between magma and host rock), as well as on whether the dykes were single or compound. This is why, in addition to their geometrical characteristics, the textural aspects of dykes need to be considered in studies that aim to understand the evolution of intrusive episodes in volcanoes.

Here, we describe the dykes cropping out at the Vicuña Pampa Volcanic Complex (VPVC), southern Central Andes. The geometrical characteristics of these dykes seem to be related to the mechanical properties of the material they intrude, but most importantly they offer a unique case study where, in a single volcanic complex, there are dykes with purely brecciated textures, purely coherent textures and with both textural domains.

Geology of the Vicuña Pampa Volcanic Complex

The Miocene Vicuña Pampa Volcanic Complex (VPVC), located at the SE margin of the Altiplano–Puna plateau (Fig. 1) and originally considered to be a collapse caldera (Rossello, 1980; Rossello and Jones, 1999; Viramonte and Petrinovic, 1999), was recently interpreted as a 30 km wide broad volcanic massif that suffered intense degradation (Guzmán *et al*., 2017).

The first volcanic cycle of the VPVC lies on top of an igneous–metamorphic basement and is formed of plugs and necks (Root Complex; 12.41 Ma), lava flows (Lower Lava Flows Succession and Upper Lava Flows Succession; 12.19 Ma) separated by a thick epiclastic succession (Cerro Morado Epiclastic Succession), block and ash flow deposits (La Cumbre Breccia) and volcanic breccias (Nacimientos Breccia) whose composition mainly ranges from basaltic andesite to andesite (Guzmán *et al*., 2017). After this first volcanic cycle, the VPVC underwent intense degradation during the middle to late Miocene that gave rise to a large morphological depression, 13–18 km wide and 1200 m deep (Guzman *et al*., 2017) (Fig. 1). The different units of the first volcanic cycle are exposed on the floor and along the walls of the depression (Fig. 1). The second volcanic cycle occurred after the main degradation of the complex, possibly during the late Miocene, and consists of block and ash deposits of the Cerro Bayo Breccia, cropping out on the SW floor of the depression (Fig. 1; Guzman *et al*., 2017).

The VPVC dykes

The VPVC units are cut by hundreds of dyke segments (Guzmán *et al.,* 2017; Carniel *et al.,* 2017) (Fig. 2). These dykes have different characteristics depending on the relative stiffness (Young's modulus, E, not measured, but qualitatively estimated) of the material they intrude: the stiffer Root Complex (see Fig. 2,3A), or the more compliant Cerro Bayo Breccia (see Fig. 2,3B), Nacimientos Breccia and undifferentiated epiclastic/volcanic material. Dykes vary in composition from basaltic (trachy)-andesites to (trachy)-andesites, with only one sampled dyke having a dacite composition (see Fig. 4 and Supplementary File 1). Dykes and other magmatic sheet intrusions are most abundant in the western portion of the depression (Fig. 2). During fieldwork we studied 33 dykes, 15 of which were sampled, recording their geographic and

stratigraphic position, textures, strike, dip and thickness (Table 1 of Supplementary File 1). More than 85% of the dykes have dip angles ranging from 60° to 90° (see Table 1 of Supplementary File 1), but moderate- to low-angle (<60°) inclined sheets are also present. Their thickness (field measurements) ranges from 0.4 m to 6 m, with an average of 1 m; their segment lengths (satellite image-based analysis) vary from 12 m to 870 m, with an average of 175 m.

Textural characteristics of the VPVC dykes

Dykes have coherent or brecciated textures, or mixtures of both. Dykes with coherent textures are mainly porphyritic and less commonly aphanitic. They have sharp contacts with the intruded rocks, without the development of glassy or quenched margins, and vary in thickness from 0.4 m to 6 m, and in dip between 35° and 88°. Porphyritic dykes are plagioclase-phyric and less frequently amphibole-phyric with cm-sized phenocrysts set in an aphanitic groundmass (Fig. 3C). Petrographically, coherent dykes show hyalocrystalline to holocrystalline inequigranular and seriate textures set in a microcrystalline (Fig. 3D), cryptocrystalline or vitric groundmass. They are basaltic (trachy)-andesite (see Supplementary File 1) and contain phenocrysts of plagioclase, clinopyroxene, orthopyroxene ± amphibole and olivine.

Dykes with brecciated textures are characterised by subangular clasts with porphyritic to aphyric textures in a matrix of the same composition (Fig. 3E,F). The clasts are trachyandesitic (phenocrysts of plagioclase, clinopyroxene, orthopyroxene ± amphibole) to dacitic with hyalocrystalline, seriate textures set in a cryptocrystalline groundmass, where minerals are smaller and frequently broken (Fig. 3F). These dykes vary in thickness from 1 m to 3 m and also show sharp contacts with the rocks they intrude. They dip between 38° and 79°.

Combinations of brecciated and coherent textural domains are sometimes found in a single or compound dyke. These mixed textures within dykes always have sharp contacts between the brecciated margins and the coherent cores or vice versa. Sometimes the contacts are sinuous (Fig. 3G,H) and one texture develops as enclaves within the other (Fig. 3G); in other cases the contacts are sharp but straight.

Dyke–host-rock thickness–texture–composition relationships

We can distinguish three groups of dykes according to their geochemical signatures (see Supplementary File 1 and groups A, B and C in Fig. 4). Small compositional variations within each group may be explained by simple processes such as different crystallization degrees. The geochemical dataset is limited (9 analyses), but we do not see a relationship between the geochemical compositions and the dyke textures (Fig. 5A), mechanical properties of the host rock (Fig. 5B), dyke thickness (Fig. 5C) or dyke dip (Fig. 5D).

We have no clear constraints on the possible variability of dyke emplacement depths, but by combining the stratigraphic relations between dykes and host rocks with geochemical analysis, we can suggest relative ages of emplacement. Since the Cerro Bayo Breccia was formed after the central depression and contains feeder dykes (Fig. 3B and 4), we infer that dykes from groups A and B (i.e. dykes intruding this and other units) are the youngest, were intruded at shallow levels (fairly close to the original topographic surface) and therefore suffered negligible erosion during arid conditions (see Guzmán *et al*., 2017). On the other hand, the only group of dykes not intruding the Cerro Bayo Breccia (group C; see Fig. 4 and Supplementary Files) may possibly have been intensely eroded after emplacement.

22 dykes intrude relatively compliant material, consisting of breccias and conglomerates. Their average thickness is 1.15 m and varies between 0.4 and 6 m (Fig. 6A), with 75% of the dykes being thinner than 3m. They dip between 35° and 90°, with 72% of them having dip angles greater than 70° (Fig. 6B). These dykes have coherent, brecciated and mixed textures with brecciated domains both in the centre and at the borders of coherent ones within a single or compound dyke (see Fig. 6C and Table 1 of Supplementary File 1).

11 dykes cut the stiffer Root Complex; their average thickness is 0.6 m and ranges between 0.5 and 2 m, with more than 80% thinner than 1 m (Fig. 6A). Their dip varies between 60° and 90°; 64% dip more than 70° (Fig. 6B). We recognised only coherent textures (Fig. 6C), of which more than 80% are porphyritic.

Discussion

The modest geochemical and mineralogical variability observed among the VPVC dykes indicates that their differences in geometry and texture cannot be attributed to contrasts in magma composition. It seems that dyke thicknesses are - at least partially - controlled by the stiffness of the intruded rocks (Fig. 7), as thicker dykes are only found cutting the relatively more compliant breccias (typical stiffness of 1–10 GPa: Gudmundsson, 2006, 2011; Gudmundsson *et al*., 2012), while thinner dykes cut both more compliant and stiffer volcanic sequences (typical stiffness up to 100 GPa: Gudmundsson, 2006, 2011; Gudmundsson *et al*., 2012). This relation matches fully the results obtained from models and previous field studies (see Keating *et al*., 2008; Geshi *et al*., 2010, 2012; Gudmundsson *et al*., 2012; Geshi and Neri, 2014; Rivalta *et al*., 2013, 2015). However, we found no dykes intruding layers with different stiffness. Furthermore,

we do not have constraints on possible differences in the local stress field and/or the load of a volcanic edifice for the different host rocks.

Dykes cutting more compliant materials show shallow dips, whereas those intruding stiffer material always have dips >60° (Fig. 6B and 7). Shallow dips may occur in dykes intruding near-surface units (e.g. Geshi *et al.,* 2010, 2012).

The brecciated nature of dykes has previously been explained as due to mechanical erosion processes - such as particle collision and wall collapse - or as related to phreato-magmatic or, more generally, an explosively driven origin (e.g. Geshi and Neri, 2014, and references therein; Vezzoli and Corazzato, 2016). Other studies show dykes with bulging and lobate margins intruding brecciated host rocks, resulting from magma propagation along a self-induced shear fault (e.g. Mathius *et al.*, 2008; Petronis *et al*., 2013); in these cases a mix of dyke breccia and crushed host rock is observed (Petronis *et al.,* 2013). We discuss here a possible explanation for the brecciated and mixed textures, based mainly on the contact relationships of domains and on their occurrence only near the surface. At the VPVC, the sharp contacts between dykes with brecciated domains and the host rock, the similar composition of clasts and matrix and the absence of pumice fragments or glass shards within the brecciated domains all seem to indicate a non-explosive origin, with a fracture mechanism similar to the one proposed by Tuffen *et al*. (2003) for tuffisites. Therefore, we invoke the possibility of brecciation during a pulsating emplacement. A sketch illustrating the different stages is presented in figure 8. This mechanism is similar to that proposed by Geshi and Oikawa (2014) for the propagation of a dyke near the topographic surface, involving, in a first stage, materials from wall-rock erosion and collapse.

These dykes may be subject to temporary arrests in response to a pressure drop when approaching the surface, causing a decrease in their temperature, which, helped by the exsolution of volatiles (Lister and Kerr, 1991), leads to drastic changes in their rheology. This can be followed by the arrival of a successive pulse of magma that, in turn, may induce fragmentation of the already almost-cooled first magma batch by exceeding its failure strength. In this case, we may see a cross section of the dyke with a brecciated portion (1st magma batch) and a remaining coherent domain (2nd magma batch; see Fig. 8A). Sometimes, usually closer to the topographic surface, the entire cross section of the dyke may be brecciated (see Fig. 8B). The time span between the emplacement of the first magma batch in the dyke and the arrival of the second batch was very short (~4.6 days for a 1 m thick dyke; see estimates in the Supplementary File 2), as the sharp and sinuous contacts and the presence of enclaves of one textural domain within the other are evidence of a ductile deformation. The few cases in which the brecciated domain is in the central portion of the dyke, and the contacts between the domains are straight, may be explained by the intrusion of a second dyke in the place where a formerly emplaced pulsating dyke was already totally solidified (Fig. 9). The new dyke uses the previous weakness zone to intrude, passing between the margins of the former dyke and the host rock, thus becoming a compound dyke. The resulting scenario shows the original central brecciated dyke enclosed by a second coherent one (Fig. 9A), with sharp but straight contacts. The proposed mechanism of formation of the brecciated textural domains (when the whole dyke is brecciated or when the brecciated domain is found at the margin of the dyke) indicates near-surface conditions.

Conclusions

At the Vicuña Pampa Volcanic Complex, dykes with three types of textures – coherent, brecciated and mixed – intrude several units of the complex with different stiffnesses. Dykes intruding stiffer materials are always coherent and tend to be thinner and more vertical; those cutting more compliant materials are generally thicker, have highly variable dip angles and can have any of the three textures. Vertical to sub-vertical dykes intrude any units regardless of their stiffness, but inclined sheets (<60°) are only present when intruding compliant materials.

The presence of dykes with brecciated and mixed textures is explained without the need to invoke explosivity or erosion of the host rock, but as a result of arrest events during dyke propagation/evolution at shallow levels; brecciated textures result when magma re-injection within semi-solidified dyke portions causes their mechanical fragmentation. Compound dykes can be generated when a second dyke intrudes along the margins of a previous solidified dyke.

Acknowledgements

SG, CML and PG are grateful for funding by ANPCyT (PICT 2012-0419; PICT 2011-0407), CONICET (PIP 489, PIP 286) and CIUNSa 1810. JM is grateful for the MECD (PRX16/00056) grant. AG is grateful for her Ramón y Cajal contract (RYC-2012-11024). S. Conway is thanked for improving the English. We acknowledge the very constructive comments made by John Browning and Thierry Menand and suggestions by the editors, Jean Braun and Agust Gudmundsson.

References

Carniel, R., Guzmán, S. and Neri, M., 2017. FIERCE: FInding volcanic ERuptive CEnters by a grid-searching algorithm in R. *Bulletin of Volcanology*, **79:**19, doi: 10.1007/s00445-017-1102-3

Browning, J. and Gudmundsson, A., 2015. Caldera faults capture and deflect inclined sheets: an alternative mechanism of ring dike formation. *Bulletin of Volcanology*, **77**:4, doi: 10.1007/s00445-014-0889-4

Daniels, K A., Kavanagh, J.L., Menand, T. and Sparks, S. J., 2012. The shapes of dikes: Evidence for the influence of cooling and inelastic deformation. *GSA Bulletin*, **124**, (7/8), 1102–1112, doi: 10.1130/B30537.1

Delcamp, A., Troll, V. R., van Wyk de Vries, B., Carracedo, J. C., Petronis, M. S., Pérez-Torrado, F. J. and Deegan, F. M., 2012. Dykes and structures of the NE rift of Tenerife, Canary Islands: a record of stabilisation and destabilisation of ocean island rift zones *Bulletin of Volcanology*, **74**, 963-980.

Ferrari, L., Garduño, V.H. and Neri, M., 1991. I dicchi della Valle del Bove, Etna: un metodo per stimare le dilatazioni di un apparato vulcanico *Mem. Soc. Geol. It*, **47**, 495-508.

Gautneb, H. and Gudmundsson, A., 1992. Effect of local and regional stress fields on sheet emplacement in West Iceland. *Journal of Volcanology and Geothermal Research*, **51**, 339-356.

Geshi, N., Kusumoto, S. and Gudmundsson, A., 2010. The geometric difference between non-feeders and feeder dikes *Geology*, **38**, 195-198, doi: 10.1130/G30350.1.

Geshi, N., Kusumoto, S., and Gudmundsson, A., 2012. Effects of mechanical layering of host rocks on dike growth and arrest *Journal of Volcanology and Geothermal Research* **223–224**, 74–82.

Geshi, N. and Neri, M., 2014. Dynamic feeder dyke systems in basaltic volcanoes: the exceptional example of the 1809 Etna eruption (Italy) *Front. Earth Sci*. **2:**13. doi: 10.3389/feart.2014.00013.

Geshi, N. and Oikawa, T., 2014. The spectrum of basaltic feeder systems from effusive lava eruption to explosive eruption at Miyakejima volcano, Japan *Bull. Volcanol.* **76**:797.doi: 10.1007/s00445-014-0797-7.

Goto, Y., Nakada, S., Kurokawa, M., Shimano, T., Sugimoto, T., Sakuma, S., Hoshizumi, H., Yoshimoto and M., Uto; K., 2008. Character and origin of lithofacies in the conduit of Unzen volcano, Japan. *Journal of Volcanology and Geothermal Research*, **175**, 45–59.

Gudmundsson, A., 1995. Infrastructure and mechanics of volcanic systems in Iceland. *Journal of Volcanology and Geothermal Research*, **64**, 1-22.

Gudmundsson, A., and Brenner, J. S., 2005. On the conditions of sheet injections and eruptions in stratovolcanoes. *Bull Volcanol*,**67**, 768-782, doi: 10. 1 007 /s00445-005-0433-7

Gudmundsson, A., 2006. How local stresses control magma-chamber ruptures, dyke injections, and eruptions in composite volcanoes *Earth Sci. Rev.*, **79**, 1–31.

Gudmundsson, A., 2011. Deflection of dykes into sills at discontinuities and magma-chamber formation *Tectonophysics*, **500**, 50-64.

Gudmundsson, A., Kusumoto, S., Simmenes, T.H., Philipp, S.L., Larsen, B. and Lotveit, I.F., 2012. Effects of overpressure variations on fracture apertures and fluid transport. *Tectonophysics*, **581**, 220–230. doi:10.1016/j.tecto.2012.05.003.

Guzmán, S., Strecker, M.R., Martí J, Petrinovic, I., Schildgen, T.F., Grosse, P, Montero-López, C., Neri, M., Carniel, R., Hongn, F.D., Muruaga, C. and Sudo, M., 2017. Construction and degradation of a broad volcanic massif: the Vicuña Pampa volcanic complex, southern Central Andes, NW Argentina. *GSA Bulletin*, in press. doi:10.1130/B31631.1

Kavanagh, J., and Sparks, R.S.J., 2011. Insights of dyke emplacement mechanics from detailed 3D dyke thickness datasets. *Journal of the Geological Society of London*, **168,** 965–978, doi:10.1144/0016-76492010-137.

Keating, G.N., Valentine, G.A., Krier, D.J. and Perry, F.V., 2008. Shallow plumbing system for small-volume basaltic volcanoes *Bull. Volcanol*., **70**, 563-582. doi: 10.1007/s00445-007-0154-1.

Le Maitre, R., Baterman, P., Dudek, A., Keller, J., Lameyre Le Bas, M., Sabine, P., Schmid, R., Sorensen, H., Streckeisen, A., Woolley, A. and Zanettin, B., 1989. A classification of igneous rocks and glossary of Terms. Blackwell, Oxford.

Lister, J.R. and Kerr, R.C., 1991. Fluid-mechanical models of crack propagation and their application to magma transport in dykes *J. Geophys. Res*., **96**, 10049-10077.

Mathieu, L., van Wyk de Vries, B., Holohan, E.P., Troll, V.R., 2008. Dykes, cups, saucers and sills: analogue experiments on magma intrusion into brittle rocks. *Earth Planet Sci Lett*, **27**, (1–4), 1–13.

McDonough, W.F. and Sun, S., 1995. The composition of the Earth. *Chem. Geol.,***120**, 223–253.

Petronis, M. S., Delcamp, A. and van Wyk de Vries, B., 2013. Magma emplacement into the Lemptégy scoria cone (Chaîne Des Puys, France) explored with structural, anisotropy of magnetic susceptibility, and Paleomagnetic data. *Bull Volcanol*, **75**, 753.

Pinel, V., and Jaupart, C., 2000. The effect of edifice load onmagma ascent beneath a volcano. *Philosophical Transactions of the Royal Society of London*, *ser. A, Mathematical and Physical Sciences*, **358**, 1515–1532, doi:10.1098/rsta.2000.0601.

Rivalta, E., Böttinger, M., Schnese, M. and Dahm, T., 2013. Supplement to: Buoyancy-driven fracture ascent: Experiments in layered gelatin. http://www.youtube.com/watch?v=8y4U1vrk-gg

Rivalta, E., Taisne, B., Bunger, A. and Katz, R., 2015. A review of mechanical models of dike propagation: Schools of thought, results and future directions *Tectonophysics*, **638**, 1-42.

Rossello, E. 1980. Nuevo Complejo Volcánico Vicuña Pampa, departamento Belén, provincia de Catamarca. *Revista de la Asociación Geológica Argentina*, **35** (3), 436-438.

Rossello, E.A, and Jones, J.P., 1999. Potencial geominero de la caldera Vicuña Pampa (27º 00'S-67º 00'W), Catamarca, in Proceedings, Congreso Geológico Argentino, 14th, Salta, **2**, 294-297.

Tuffen, H., Dingwell, D.B. and Pinkerton, H., 2003. Repeated fracture and healing of silicic magma generate flow banding and earthquakes? Geology, **31**, 1089–1092.

Vezzoli, L. and Corazzato, C., 2016. Volcaniclastic dykes tell on fracturing, explosive eruption and lateral collapse at Stromboli volcano (Italy) *Journal of Volcanology and Geothermal Research*, **318**, 55–72.

Viramonte, J.G., and Petrinovic, I.A., 1999. La caldera de Culampajá: una caldera basáltica en la Puna Austral, in Proceedings, Congreso Geológico Argentino, 14th, Salta, **2**, 235.

Figure captions

Fig. 1: Geological map of the Vicuña Pampa Volcanic Complex. Modified from Guzman *et al.* (2017).

Fig. 2: Dyke distribution within the VPVC, differentiating the units they intrude and their textures (for the 33 dykes described in the field).

Fig. 3: A) Dykes – dotted white lines along margins – intruding the Root Complex (stiff material; note person (circled) for scale). B) Dykes – dotted white lines along margins – cutting the Cerro Bayo Breccia (relatively compliant material), and a small lava flow above the Cerro Bayo Breccia – continuous white line. C) Dyke with coherent plagioclase-phyric texture (see dyke 1 in Table 1 in Supplementary File 1). D) Microphotograph of a dyke with porphyric texture and microcrystalline matrix. E) Dyke with brecciated texture (see dyke 8 in Table 1 in Supplementary File 1); dashed black lines indicate the borders of some fragments within the breccia. F) Microphotograph of a brecciated dyke; dashed yellow lines indicate the borders of some fragments within the breccia. G) Dyke with mixed texture (dyke 33 in Table 1 in Supplementary File 1); the margin shows a brecciated texture (Br) and displays a sharp-ductile contact (black line) with the coherent (Coh) porphyric inner domain; note (circle) that some portions of the porphyric domain are included in the brecciated domain. H) Microphotograph of the dyke in Fig. 3G; brecciated (Br) and coherent (Coh) porphyric textures separated by a sharp and sinuous contact (dashed yellow line).

Fig. 4: A) General sketch of the stratigraphic relations between dykes and host rocks; colours indicate the different geochemical groups of dykes. Note that dykes from groups A and B cut the Cerro Bayo Breccia (CBB; post-depression unit) and other units, and those from group C cut the older Root Complex and undifferentiated volcanic/epiclastic deposits (pre-depression units). Vertical prolongation of dykes is represented by dashed lines (black for pre-main-degradation intrusions and grey for post-Cerro Bayo Breccia) indicating the possible original locations of their tips; B,C) Main evidence to discriminate geochemical groups of dykes; differences in major elements may be related to variable degrees of crystal fractionation. B) Total Alkalis Silica diagram (Le Maitre *et al.,* 1989); C) Ba/Th vs Eu/Eu* diagram. D–F) Chondrite-normalised diagrams (McDonough and Sun, 1995) of D) dykes from group A, E) dykes from group B and F) dykes from group C.

Fig. 5: Harker diagrams of Zr (ppm) vs Sr (ppm) as a function of: A) textures, B) stiffness of intruded material, C) dyke thickness, and D) dyke dip. Colours indicate geochemical groups as in Fig. 4.

Fig. 6: Histograms of (A) dyke thickness, (B) dip and (C) texture as a function of host-rock stiffness.

Fig. 7: Thickness versus dip of dykes in relation to the stiffness of the units they intrude.

Fig. 8: Schematic interpretation of a pulsating dyke; t_1, t_2 and t_3 indicate three stages during the formation of a single pulsating dyke. In t_1, the first magma batch is emplaced; in t_2, the second magma batch intrudes, producing upward pressure (black arrows) and consequent fragmentation of the first magma batch; t_3 shows the final result: a coherent core and brecciated margins

separated by sharp and sinuous contacts. A) Portion with brecciated margin and coherent core; the limit between textural domains is marked by a black line, as are small enclaves of the coherent domain inside the brecciated one; some enclaves of the brecciated domain inside the coherent one are highlighted in grey. B) Brecciated portion of a dyke.

Fig. 9: Schematic interpretation of a compound dyke, formed by an inner pulsating dyke (see schematic process in Fig. 8) plus an outer single dyke emplaced along the margins; note the inner brecciated domain is contained and wrapped by the external coherent domain.

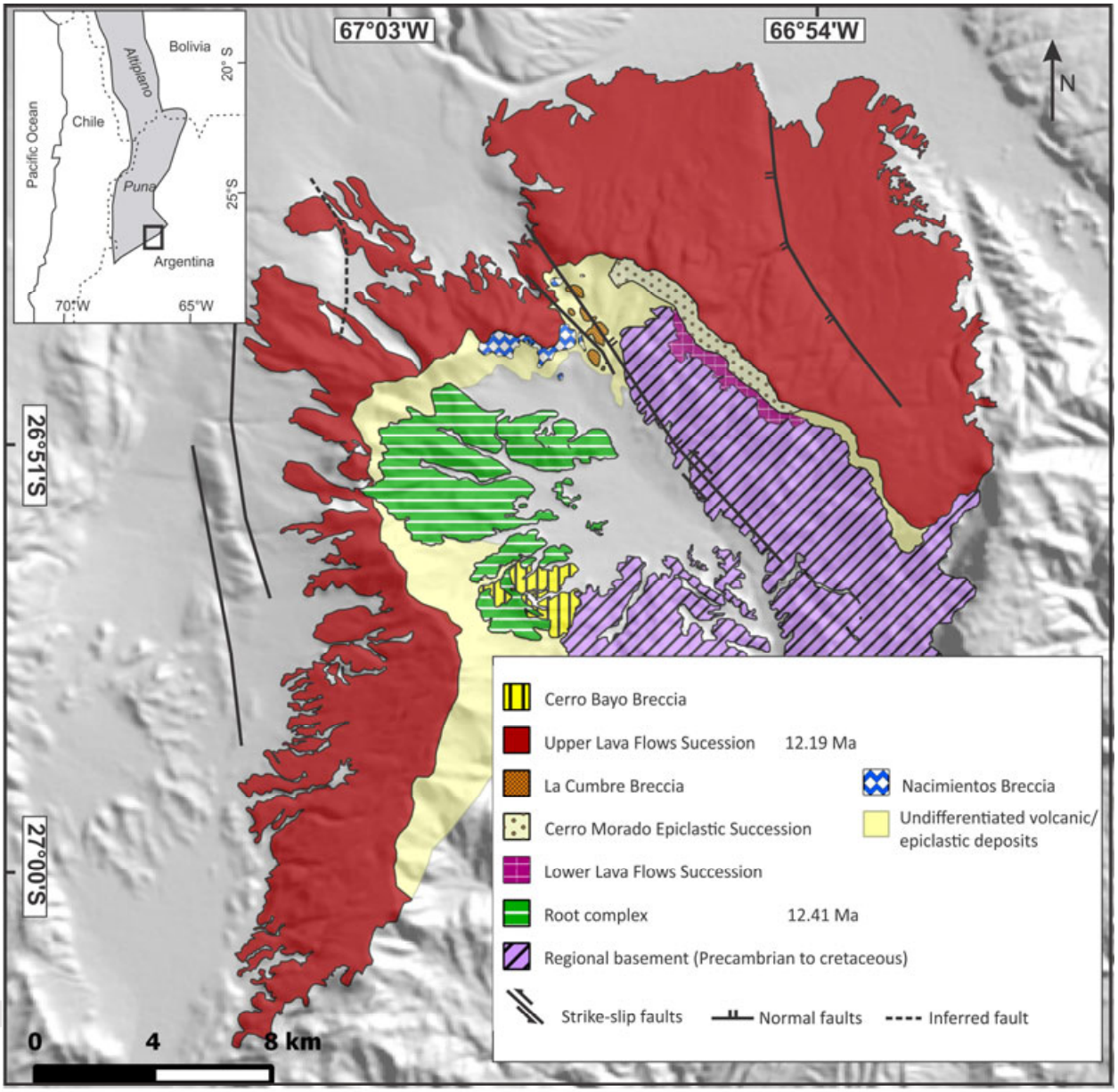

Fig.1

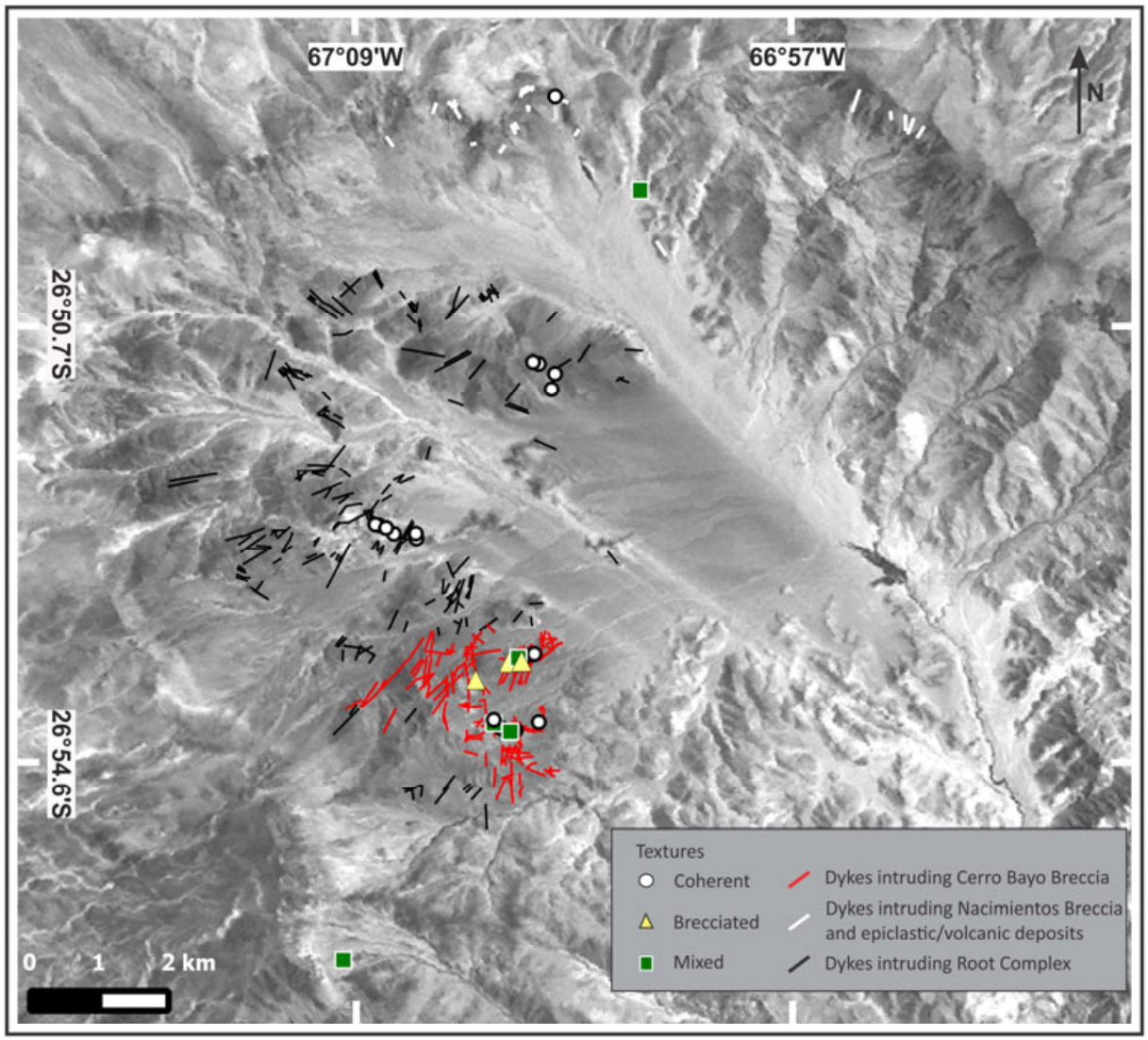

Fig. 2

Fig. 3

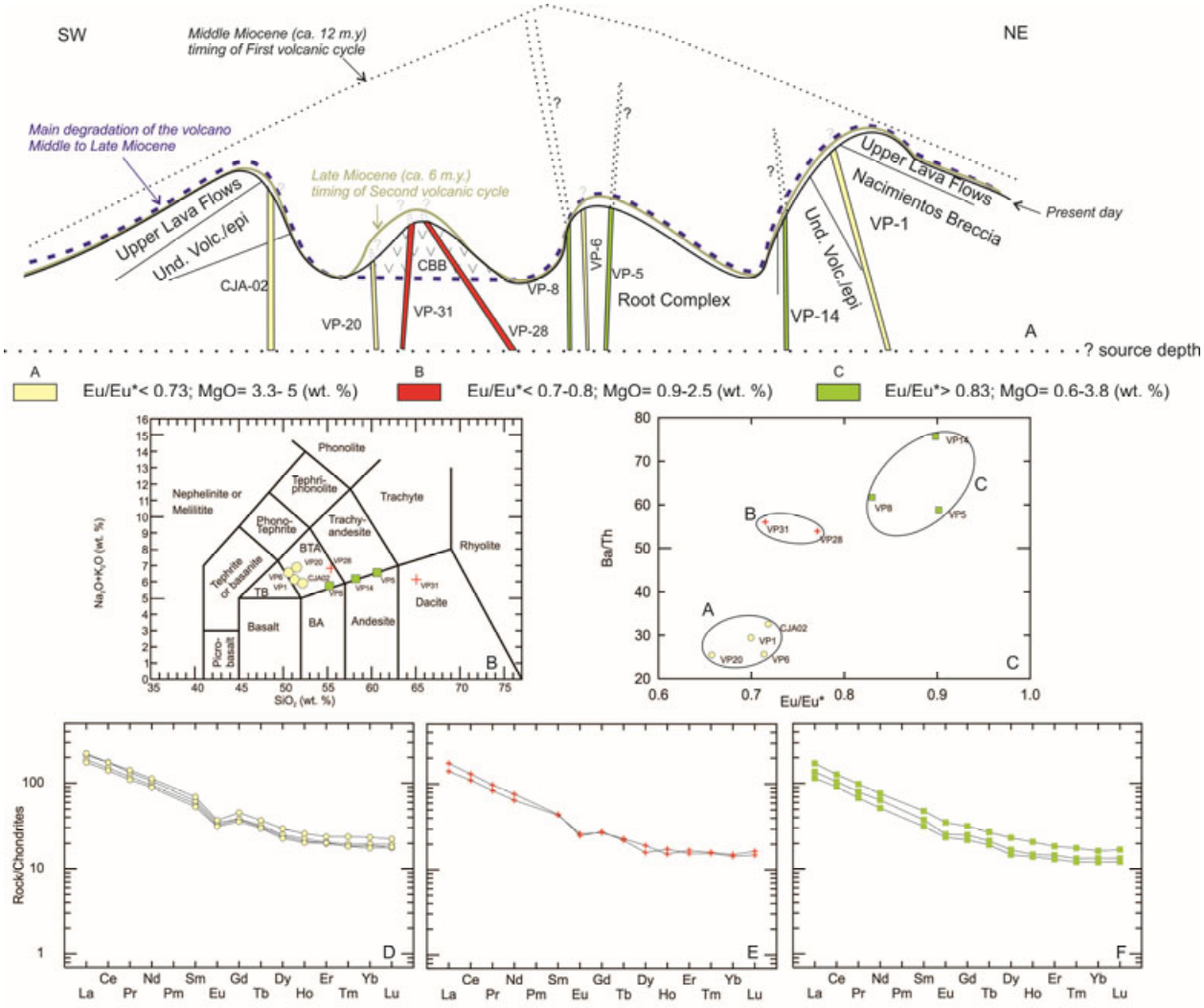

Fig. 4

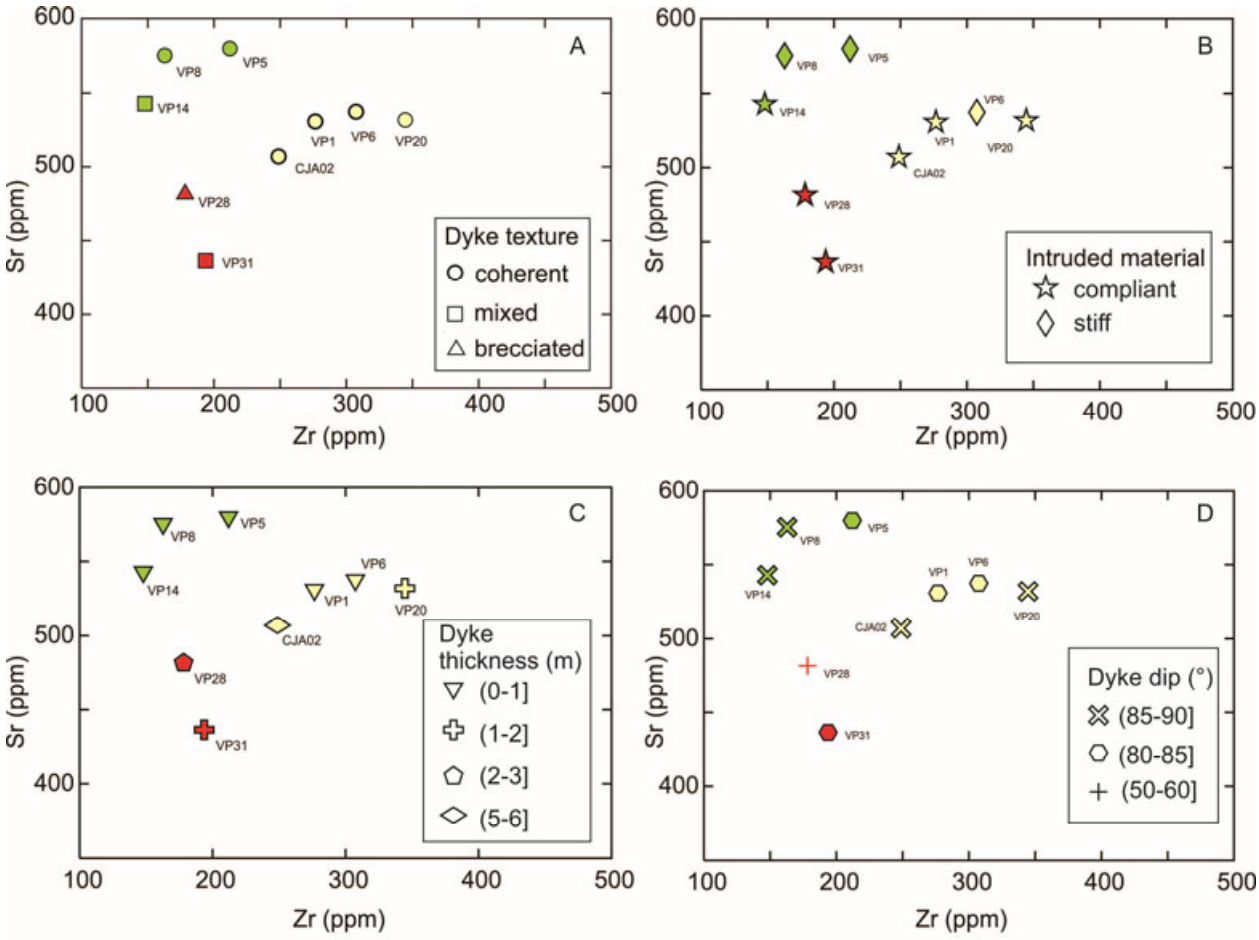

Fig.5

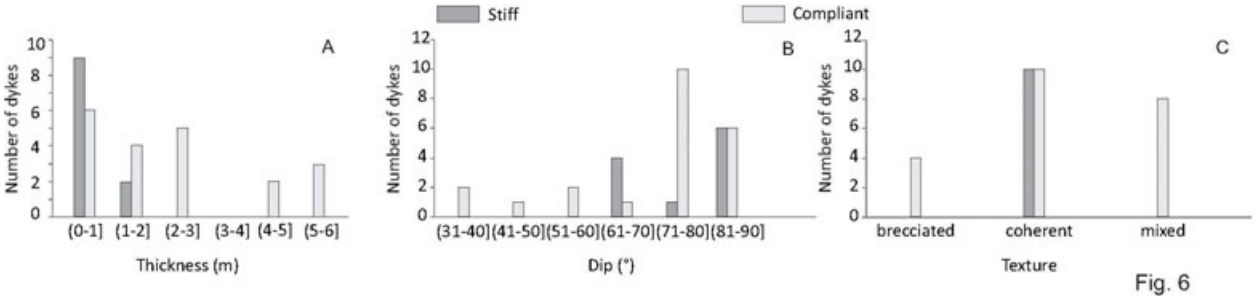

Fig. 6

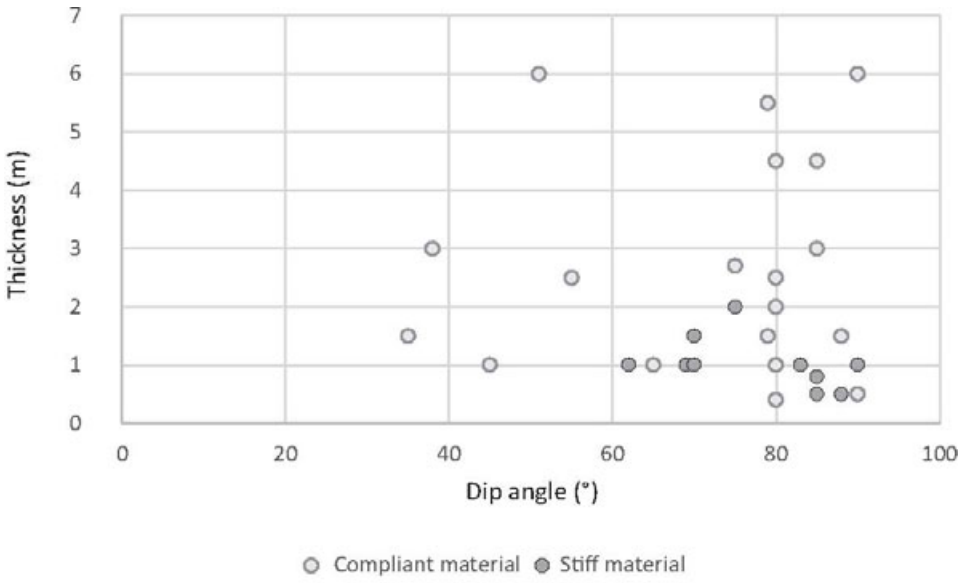

Fig. 7

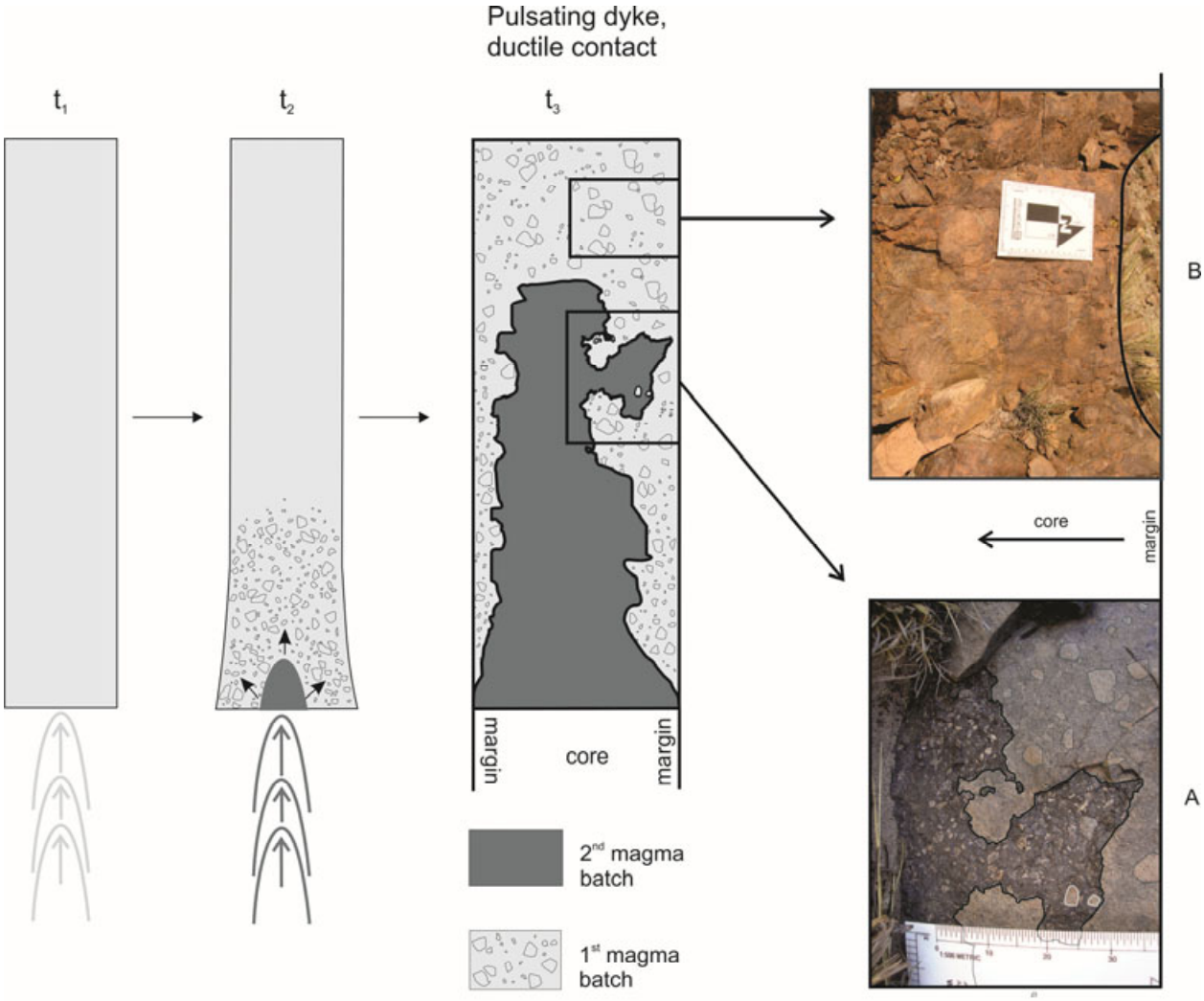

Fig. 8

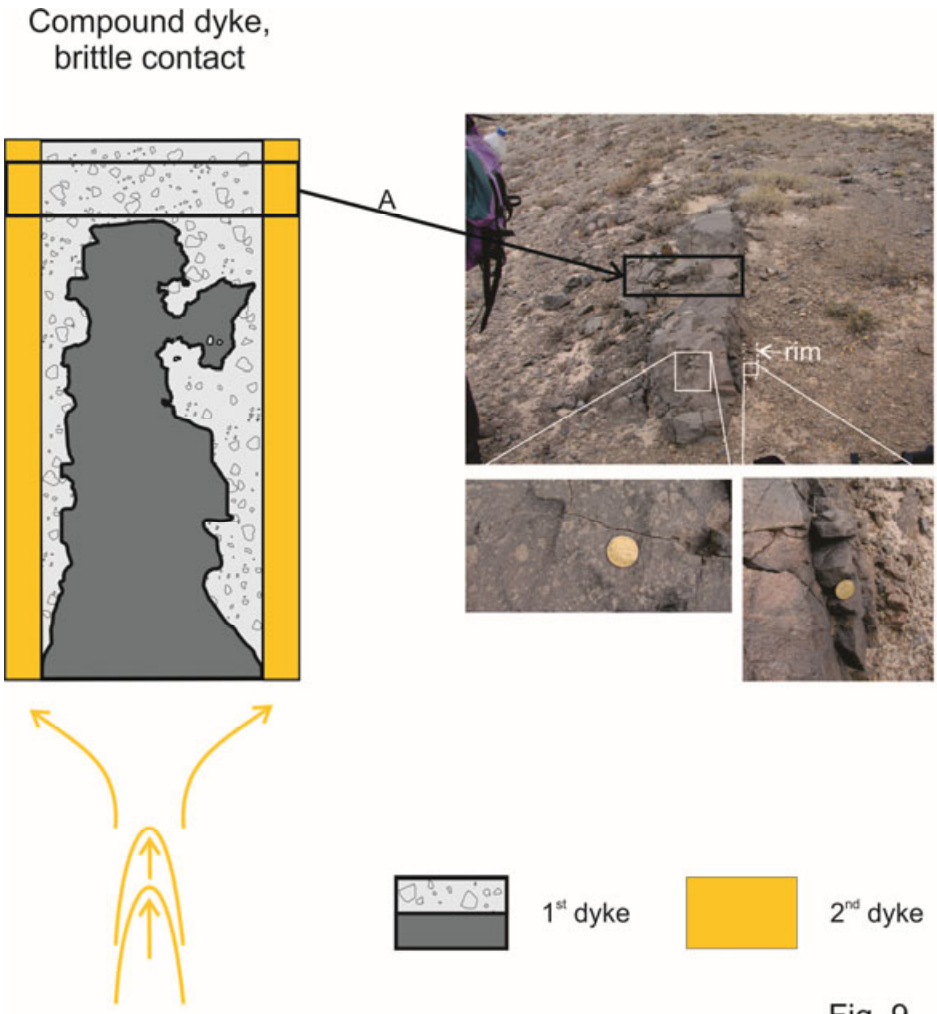

Fig. 9